Chemical Engineering Journal 178 (2011) 443–450

Contents lists available at SciVerse ScienceDirect

Chemical Engineering Journal

journal homepage: www.elsevier.com/locate/cej

Preparation of core–shell magnetic ion-imprinted polymer for selective extraction of Pb(II) from environmental samples

Minglei Zhang [a], Zhaohui Zhang [a,b,c,*], Yunan Liu [a], Xiao Yang [a], Lijuan Luo [a], Jutao Chen [a], Shouzhuo Yao [b]

[a] College of Chemistry and Chemical Engineering, Jishou University, Jishou 416000, China
[b] State Key Laboratory of Chemo/Biosensing and Chemometrics, Hunan University, Changsha 410082, China
[c] Research Center for Eco-Environmental Sciences, Chinese Academy of Sciences, Beijing 100085, China

ARTICLE INFO

Article history:
Received 28 June 2011
Received in revised form 6 October 2011
Accepted 11 October 2011

Keywords:
Core–shell
Fe_3O_4@SiO_2@IIP
Pb(II)
M-SPE

ABSTRACT

A novel magnetic ion-imprinted polymer (Fe_3O_4@SiO_2@IIP) was synthesized by using 3-(2-aminoethylamino)propyltrimethoxysilane (AAPTS) as the functional monomer, tetraethylorthosilicate (TEOS) as the cross-linker and Pb(II) as the template and evaluated for selective extraction of Pb(II) from environmental sample by magnetic solid phase extraction (M-SPE) procedure. The factors affecting separation and preconcentration of the target heavy metals involving pH, eluting solvent and sample volume were studied in detail. Under the optimized experimental conditions, the kinetics adsorption and adsorption capacity of the Fe_3O_4@SiO_2@IIP toward Pb(II) were estimated. The results indicated that the adsorption mechanism is corresponding with the second-order adsorption process with correlation coefficient ($r^2 = 0.990$), and the maximum adsorption capacity is 19.61 mg g^{-1}. The relative selectivity factor (β) values of Pb(II)/Cu(II), Pb(II)/Zn(II), Pb(II)/Cd(II) and Pb(II)/Hg(II) are 7.41, 6.76, 3.75 and 6.39, respectively. The Fe_3O_4@SiO_2@IIP was applied for extracting and detecting of Pb(II) in real environmental samples combined with atomic adsorption spectrometer successfully with high recoveries of 98.0%.

1. Introduction

Solid phase extraction (SPE) is a well-established method for sample clean-up and preconcentration in the analysis of biological and environmental samples because of its advantages involving convenience, time-saving and simplicity [1]. Nowadays, SPE combined with magnetic sorbents (M-SPE) has got increasing attention. Compared with conventional sorbents, magnetic sorbents possess large surface area and short diffusion route, which resulted in high extraction efficiency and rapid extraction dynamics [2–5].

Over the past few decades, Fe_3O_4 particles, one of magnetic particles, have attracted worldwide attention because of their unique physical and chemical properties, biocompatibility and remarkable magnetic properties [6–9]. However, the traditional coating of Fe_3O_4 particles cannot separate analytes efficiently from the complex biological or environmental samples. Fortunately, a method combining Fe_3O_4 particles with molecularly imprinted polymer (Fe_3O_4@MIP) for extracting analytes from complex samples was developed [10–14]. MIP is a synthetic material which can selectively recognize the template molecule from related analogous compounds, and have been investigated as highly selective sorbents for SPE to concentrate and clean up samples prior to analysis [15,16]. Similar to MIP, ion-imprinted polymer (IIP) as selective sorbents for a particular chemical element, have received much attention [17,18]. Due to the advantageous properties such as high mass transfer rates and good fluid–solid contact of magnetic Fe_3O_4, more and more researchers used it as carriers to prepare core–shell IIP [19–21]. However, surface modification or coating of Fe_3O_4 particles to get strong magnetic and uniform imprinted polymer particles are the key challenge for these applications.

Recently, surface imprinting by sol–gel process has been successfully applied for the imprinted coating on silica gel [22,23], multi-wall carbon nanotubes [24] and magnetic particles [10–14,19–21]. However, the limited functional silica monomers restrict the development of surface imprinting by sol–gel process. Up to now, most of these core–shell imprinted materials were used to extract heavy metal ions involving Hg(II), Cd(II), Ni(II), and Cu(II) because of their significant threat to the ecosystem and especially to people due to the severe toxicological effects on living organisms [25–27]. Lead, as one of the most toxic heavy metal elements, can transferred into animals and human beings through the food chain, and result in ecological and health toxic effects even at very low concentrations [28]. However, few researches on using 3-(2-aminoethylamino)propyltrimethoxysilane (AAPTS) as functional ligand to prepare ion-imprinted materials for extraction of lead ion from environmental samples have been reported.

* Corresponding author. Tel.: +86 743 8563911; fax: +86 743 8563911.
E-mail address: zhaohuizhang77@163.com (Z. Zhang).

1385-8947/$ – see front matter © 2011 Elsevier B.V. All rights reserved.
doi:10.1016/j.cej.2011.10.035

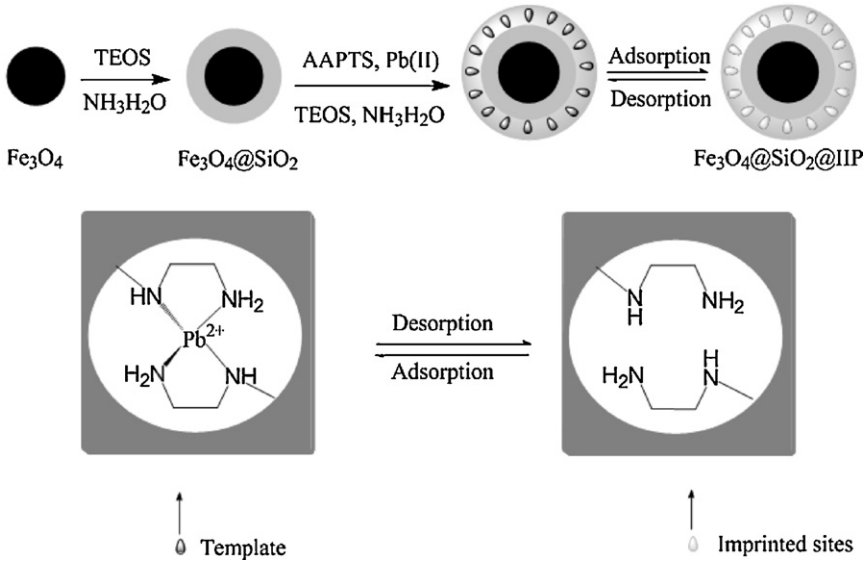

Fig. 1. Schematic expression of synthesis of Fe_3O_4@SiO_2@IIP.

In our work, a core–shell magnetic ion-imprinted polymer (Fe_3O_4@SiO_2@IIP) was synthesized with surface imprinting technique. The Fe_3O_4@SiO_2@IIP was prepared under catalysis of ammonia water using Fe_3O_4@SiO_2 as the support, lead ion as the template, AAPTS as the functional monomer, and tetraethyl orthosilicate (TEOS) as the cross-linker. The obtained product was characterized by SEM, IR and XRD, and the adsorption performance and application were studied in detail.

2. Materials and methods

2.1. Materials and chemicals

Tetraethylorthosilicate (TEOS) was purchased from Sigma. 3-(2-Aminoethylamino)propyltrimethoxysilane (AAPTS) was obtained from Aldrich. $Pb(NO_3)_2$, $FeCl_3{\cdot}6H_2O$, NaAc, ethylene glycol and polyethylene glycol 4000 (PEG) were purchased from Changsha Chemical Reagent Company (Hunan, China). All reagents used were of analytical grade.

2.2. Instrumentation

FT-IR spectrums between 400 cm^{-1} and 4000 cm^{-1} of Fe_3O_4, Fe_3O_4@SiO_2@IIP and Fe_3O_4@SiO_2@NIP were obtained by an IMPACT-400 FT-IR Analyzer. The morphologies of Fe_3O_4, Fe_3O_4@SiO_2 and Fe_3O_4@SiO_2@IIP were investigated by using JSM-6700F scanning electron microscope. The samples of Fe_3O_4 and Fe_3O_4@SiO_2@IIP were characterized by X-ray diffractometer (Y2000, Dandong Aolong Radiative Instrument Co., Ltd, China) operating with a Cu anode at 40 kV and 50 mA in the range of 2θ value between 10° and 80° with a speed of 3° min^{-1}. Magnetic measurements were carried out using a vibrating sample magnetometer (VSM, 7300, Lakeshore) under a magnetic field up to 10 kOe. In M-SPE procedure, the magnetic adsorbent (Fe_3O_4@SiO_2@IIP or Fe_3O_4@SiO_2@NIP) was firstly dispersed in the real samples (after pretreatment) of tap water, lake water and surface river water. After the adsorption was saturated, the magnetic adsorbent was separated with the help of an external magnetic force, and washed with water. Finally, the magnetic adsorbent was eluted with certain volume of eluting solvent, and the eluting solution was collected for further determination. A flame atomic absorption spectrometer (AA-6500, Shimadzu, Japan) with air-acetylene burner and a single element hollow cathode lamp was used to detect the metal ions concentration.

2.3. Preparation of Fe_3O_4@SiO_2@IIP

2.3.1. Synthesis of magnetic Fe_3O_4 particles

The magnetic Fe_3O_4 particles were synthesized according to previous report [29]. Briefly, $FeCl_3{\cdot}6H_2O$ (1.35 g) and NaAc (3.6 g) were dissolved in 50 mL of ethylene glycol under magnetic stirring until the reactants were dissolved completely. This mixture solution was purged with N_2 for 10 min, and then transferred to a Teflon-lined stainless-steel autoclave and sealed to heat at 200 °C for 8 h. After the autoclave was cooled to ambient temperature, the obtained black magnetic Fe_3O_4 particles were washed with ethanol, and then dried in vacuum at 60 °C for 12 h.

2.3.2. Synthesis of Fe_3O_4@SiO_2

Fe_3O_4 particles (0.10 g) were firstly treated by HCl solution (50.0 mL, 1.0 mol L^{-1}) under ultrasonic vibration for 10 min. Then the magnetic Fe_3O_4 particles were separated with the help of an external magnetic force and thoroughly washed with deionized water, and redispersed in ethanol (150 mL). Concentrated ammonia aqueous solution (12 mL, 25 wt%) and TEOS (100 μL) were added in succession and the suspension was left in an ice bath for 2 h under ultrasonic vibration. The obtained Fe_3O_4@SiO_2 was separated with the help of an external magnetic force, and washed with water and ethanol, respectively.

2.3.3. Preparation of Fe_3O_4@SiO_2@IIP

Fe_3O_4@SiO_2@MIP was prepared with a sol–gel process and the schematic expression of synthesis of Fe_3O_4@SiO_2@IIP was shown in Fig. 1. Briefly, $Pb(NO_3)_2$ (0.15 g) and AAPTS (200 μL) were dispersed in the mixture solution of ethanol (80 mL) and deionized water (60 mL) under ultrasonic vibration. Then, TEOS (400 μL), Fe_3O_4@SiO_2 (0.1 g) and concentrated ammonia aqueous solution (1.0 mL, 28 wt%) were sequentially added into the above solution under ultrasonic vibration. The polymerization reaction was carried out at room temperature under stirring for 6 h with mechanical agitating to obtain the particles with a high cross-linking structure. Finally, the product was separated with the help of an external magnetic force, and washed with water and ethanol in succession.

In order to remove Pb(II), the polymer was treated with 50 mL of 0.2 mol L^{-1} HNO_3 under slightly shaking for three times. The obtained Fe_3O_4@SiO_2@MIP was washed with water, and then dried in vacuum oven at 60 °C for 24 h.

Magnetic non-imprinted polymer (Fe_3O_4@SiO_2@NIP) was prepared following the same procedure without adding $Pb(NO_3)_2$.

2.4. Batch adsorption experiments

Batch adsorption experiments of the Fe_3O_4@SiO_2@IIP and Fe_3O_4@SiO_2@NIP were preformed in aqueous solution. Respective polymers (20 mg) were equilibrated with 5 mL of deionized water (pH = 7.5) spiked with Pb(II) at room temperature for 1 h under slightly shaking. Then the Fe_3O_4@SiO_2@IIP was collected with the help of an external magnetic force. The supernatant was analyzed using flame atomic absorption spectrometer (FAAS). The amount of Pb(II) bound by the polymer was calculated according to the following formula:

$$Q = \frac{(C_0 - C)V}{1000W}$$

where Q is the amount of Pb(II) adsorbed (mg g^{-1}); C_0 and C are the initial and final concentration of Pb(II) (μg mL^{-1}), respectively; V is the volume of mixture (mL); W is the amount of polymer (g). All the tests were carried out in triplicate.

2.5. Sample preparation

The tap water (Waterworks, Jishou City), lake water (Fengyu Lake, Jishou City) and surface river water (Dong River, Hunan) samples were collected locally. Prior to sampling, the bottles were cleaned with deionized water, diluted nitric acid and deionized water in succession. The samples were immediately filtered through a cellulose filter membrane (pore size 0.45 μm). After acidification with HNO_3, the samples were stored at 4 °C. The pH of samples was adjusted with ammonium hydroxide and acetic acid solution before determination.

3. Results and discussion

3.1. Preparation of Fe_3O_4@SiO_2@IIP

In this work, the surface imprinting and sol–gel technique were combined to prepare the Fe_3O_4@SiO_2@IIP. Prior to coating imprinted layer on the surface of Fe_3O_4, modification of Fe_3O_4 is necessary. In the first step, sol–gel approach was used to deposit silica on the surface of Fe_3O_4 particles. In the second step, AAPTS was used as functional ligand for the surface imprinting of lead ion on the modified Fe_3O_4. Due to the presence of the functional group of –NH–CH_2–CH_2–NH_2, AAPTS can form coordination effect with Pb(II) [27]. First, certain amount of AAPTS was added into methanol solution containing certain amount of Pb(II), and a turbid solution was observed immediately. Second, deionized water was added continuously into the mixture solution. It is worth noting that when the volume ratio between methanol and water was 4:3, the mixture solution became clear completely. Finally, TEOS and Fe_3O_4@SiO_2 were added, and the polymerization was conducted under the catalysis of concentrated ammonia aqueous solution.

3.2. Characteristics

The morphologies of Fe_3O_4 and Fe_3O_4@SiO_2@IIP were characterized with scanning electron microscopy. As shown in Fig. 2, the particles size of Fe_3O_4, Fe_3O_4@SiO_2 and Fe_3O_4@SiO_2@IIP were about 100 nm, 150 nm and 200 nm, respectively. Thus the imprinted shell was about 25 nm by calculating.

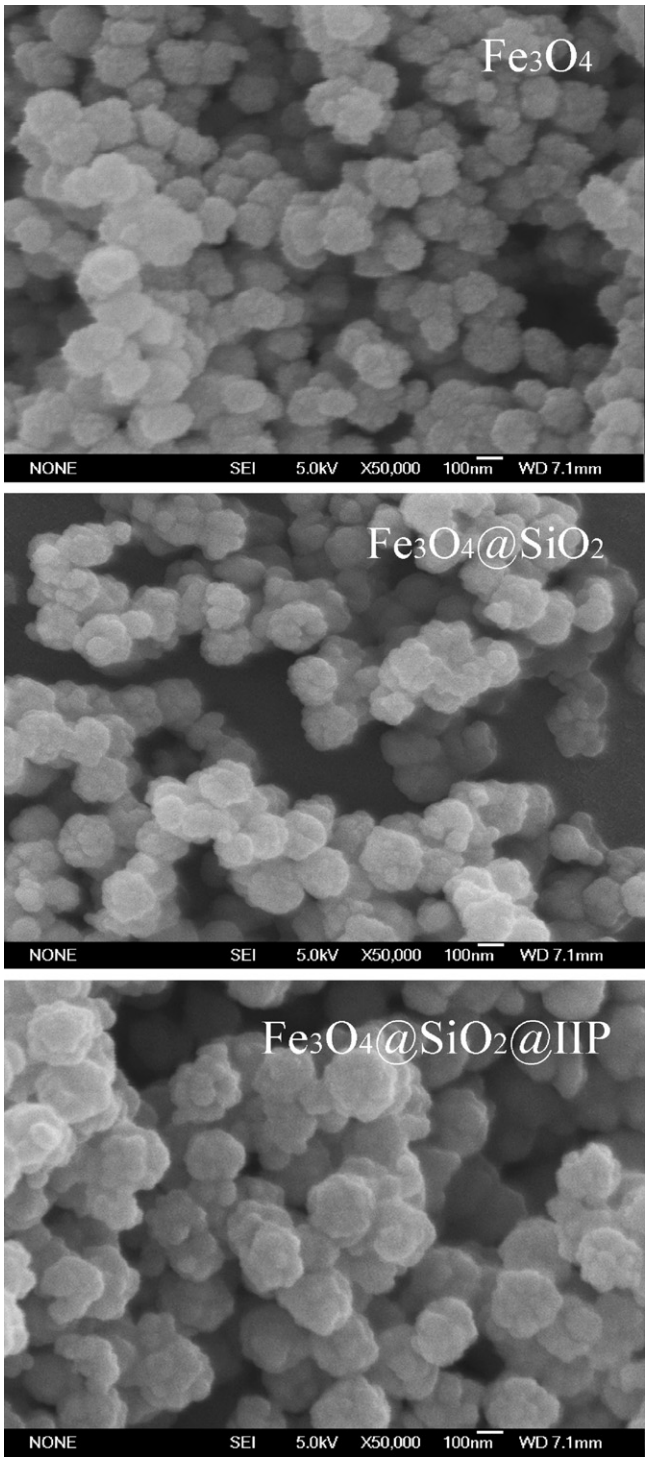

Fig. 2. SEM images of Fe_3O_4, Fe_3O_4@SiO_2 and Fe_3O_4@SiO_2@IIP.

FT-IR spectroscopy was used to study the chemical structure of the Fe_3O_4@SiO_2@IIP. The results were shown in Fig. 3. A sharp and strong peak at 590 cm^{-1} corresponding to the stretching Fe–O was observed in all the samples [22], which indicated the Fe_3O_4 particles were encapsulated inside of the Fe_3O_4@SiO_2@IIP. The peaks at 1384 cm^{-1} and 3420 cm^{-1} corresponded to the stretching vibration of CH_2–N and O–H in both Fe_3O_4@SiO_2@IIP samples. It was notable that the peak of CH_2–N in Fe_3O_4@SiO_2@IIP loading with Pb(II) was stronger than that without loading with Pb(II), which was attributed to the formation of coordination effect between AAPTS and Pb(II). The differences of FT-IR in both Fe_3O_4@SiO_2@IIP samples

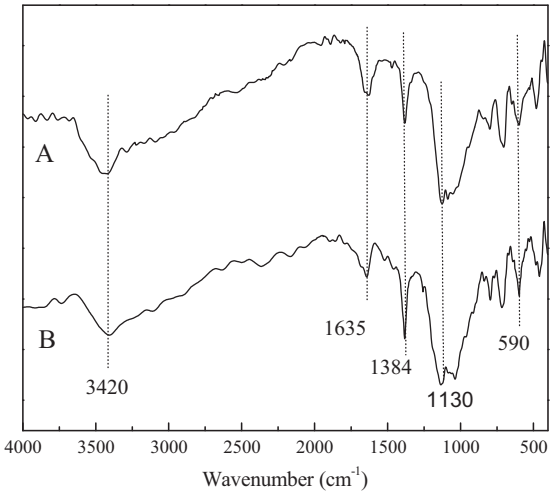

Fig. 3. FT-IR spectrums of Fe_3O_4@SiO_2@IIP without loading Pb(II) (A) and Fe_3O_4@SiO_2@IIP loaded with Pb(II) (B).

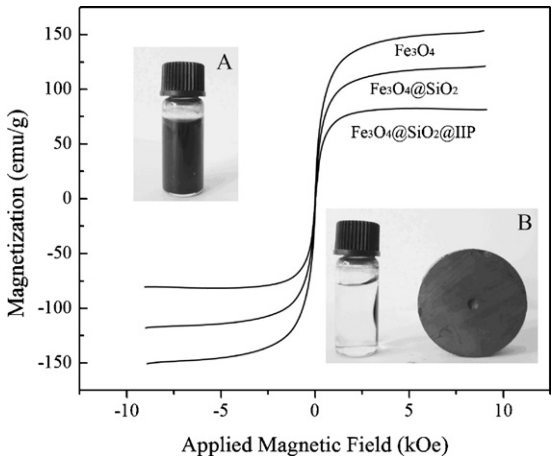

Fig. 5. Magnetization curves at room temperature of the synthesized Fe_3O_4, Fe_3O_4@SiO_2 and Fe_3O_4@SiO_2@IIP; digital photographs of the Pb(II) solution with dispersed Fe_3O_4@SiO_2@IIP (A) and the Pb(II) solution after magnetic separation with the help of an external magnetic field (B).

indicated that the Pb(II) imprinted layer was coated on the Fe_3O_4 particles successfully [25].

As shown in Fig. 4, six diffraction peaks for Fe_3O_4 can be indexed to (2 2 0), (3 1 1), (4 0 0), (4 2 2), (5 1 1) and (4 4 0), which match well with the database of magnetite in JCPDS (JCPDS Card No. 19-629) file. All peaks of Fe_3O_4@SiO_2@IIP are almost the same as Fe_3O_4, which revealed that the surface-modified Fe_3O_4 particles did not lead to their phase change.

For M-SPE procedure, it is important that the Fe_3O_4@SiO_2@IIP should possess sufficient magnetic attraction for magnetic separation in practical application. Therefore, the magnetic properties of the Fe_3O_4, Fe_3O_4@SiO_2 and Fe_3O_4@SiO_2@IIP were analyzed by VSM at room temperature, and the magnetic hysteresis curves were shown in Fig. 5. Compared with Fe_3O_4, the saturation magnetization of Fe_3O_4@SiO_2@IIP decreased somewhat, which is due to Fe_3O_4@SiO_2@IIP coating with SiO_2 and imprinted layer. However, with such high saturation magnetization, as shown in Fig. 5, the Fe_3O_4@SiO_2@IIP could easily and quickly be separated from a suspension. A dark homogeneous dispersion with dispersed Fe_3O_4@SiO_2@IIP was observed in the absence of an external magnetic field, while black imprinted particles were attracted on the internal wall of vial and the dispersion became clear immediately with the help of an external magnetic field. The results indicated that the Fe_3O_4@SiO_2@IIP could be applied to M-SPE procedure.

3.3. Adsorption behaviors of imprinted sorbent

3.3.1. Effect of pH on the adsorption of Pb(II)

It is well known that pH plays an important role in adsorption performance of the imprinted polymer toward different ions [30]. The effect of pH on the adsorption of Fe_3O_4@SiO_2@IIP toward Pb(II) was studied with varying the pH from 4.0 to 9.0 and the results were presented in Fig. 6. The results showed that the adsorption percentage of Pb(II) increased with the increasing pH of the aqueous solution from 4.0 to 7.5, then remained constant with further increase in pH from 7.5 to 9.0. The adsorption mechanism of Pb(II) could be explained by the coordination effect between AAPTS and Pb(II) [25]. At lower pH, adsorption of Pb(II) is very low due to the protonation of –NH–CH_2–CH_2–NH_2; when the pH was higher than 7.5, high adsorption percentage was obtained as a result of no protonation of –NH–CH_2–CH_2–NH_2. Thus all samples were adjusted to pH 7.5 for further studies.

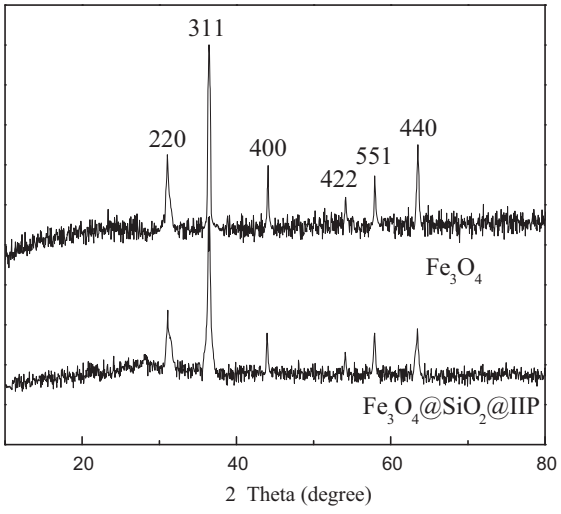

Fig. 4. XRD patterns for Fe_3O_4 and Fe_3O_4@SiO_2@IIP.

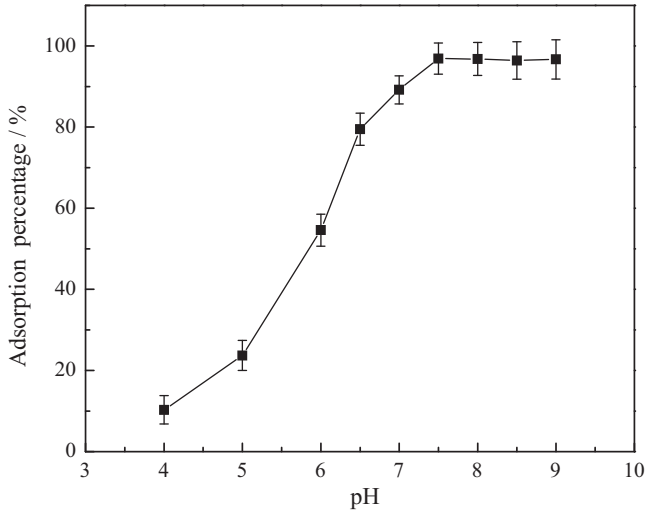

Fig. 6. Effect of pH on adsorption capacity of Fe_3O_4@SiO_2@IIP.

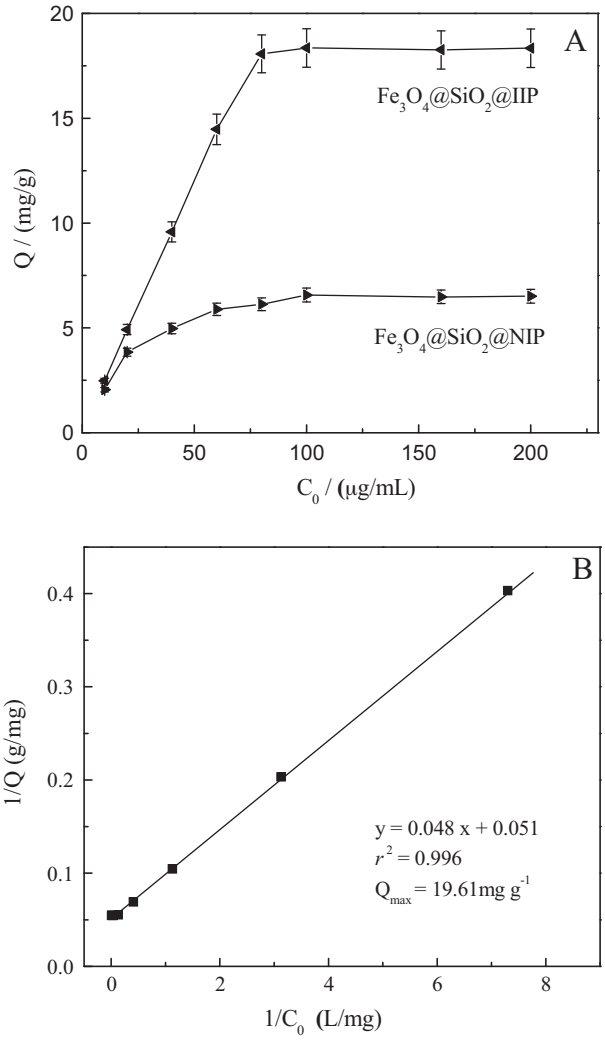

Fig. 7. Adsorption capacities of Fe_3O_4@SiO_2@IIP and Fe_3O_4@SiO_2@NIP (A), fitted Langmuir equation of Fe_3O_4@SiO_2@IIP (B).

3.3.2. Evaluation of adsorption capacity

The adsorption capacity of the Fe_3O_4@SiO_2@IIP toward Pb(II) was investigated by batch experiments. As shown in Fig. 7(A), the adsorption capacity increased with the increasing initial concentration of Pb(II) solution when the concentration is less than 75 μg/Ml, which can be explained that the specific binding sites were not saturated at lower concentration of Pb(II). While the specific binding sites were completely occupied at higher Pb(II) concentration. Owing to the specific binding sites in the imprinted shell, the Fe_3O_4@SiO_2@IIP exhibited a good imprinted effect for Pb(II), and the adsorption capacity of the Fe_3O_4@SiO_2@IIP toward to Pb(II) is up to 18.35 mg g^{-1}. In addition, the adsorption capacity of the Fe_3O_4@SiO_2@NIP toward Pb(II) was 6.57 mg g^{-1}, which was less than that of Fe_3O_4@SiO_2@IIP. This can be explained that the presence of the functional group of –NH–CH_2–CH_2–NH_2 on the surface of Fe_3O_4@SiO_2@NIP can absorb Pb(II) by coordination effect [27].

During the batch experiments, the adsorption equilibrium of Pb(II) on Fe_3O_4@SiO_2@IIP was fitted to Langmuir equation:

$$\frac{1}{q_e} = \frac{1}{Q_{max}} + \frac{1}{bQ_{max}C_e}$$

where q_e (mg g^{-1}) is the equilibrium adsorbed amount of Pb(II), Q_{max} (mg g^{-1}) is the maximum adsorption capacity, C_e (mg L^{-1}) is the equilibrium concentration, and b (L mg^{-1}) is the adsorption equilibrium constant. The correlation coefficient (r^2) and the maximum adsorption capacity (Q_{max}) was calculated as 0.989 and 19.61 mg g^{-1} from Fig. 7(B).

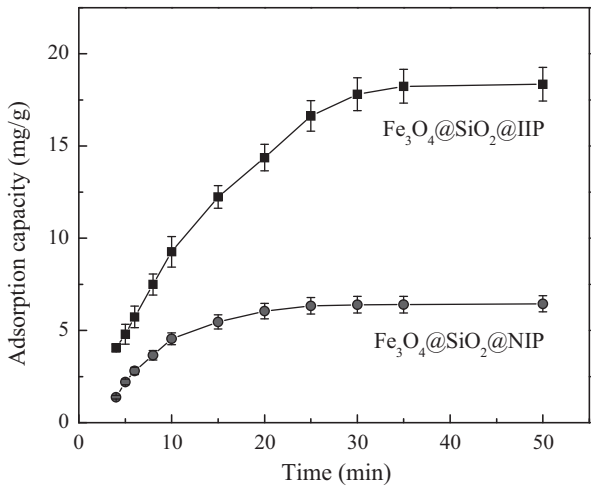

Fig. 8. Adsorption rate of Pb(II) on Fe_3O_4@SiO_2@IIP and Fe_3O_4@SiO_2@NIP (Fe_3O_4@SiO_2@IIP amount 20 mg; Pb(II) 100 μg mL^{-1}; pH 7.5; sample volume of 5 mL).

3.3.3. Adsorption kinetic

Kinetic adsorption experiments of Pb(II) on the Fe_3O_4@SiO_2@IIP and Fe_3O_4@SiO_2@NIP were conducted in aqueous solution by a batch system. In total, 20 mg of the imprinted sorbent was added to 5 mL of 100 μg L^{-1} Pb(II) aqueous solution at pH 7.5. It can be seen that a much higher adsorption capacity was achieved on Fe_3O_4@SiO_2@IIP from Fig. 8. And the velocity of adsorption of the Fe_3O_4@SiO_2@IIP is fairly rapid and saturation adsorption can be obtained within 35 min, which can be attributed to the high coordination effect between –NH–CH_2–CH_2–NH_2 and Pb(II).

Moreover, the pseudo first-order and pseudo second-order kinetic models were used to investigate the kinetic mechanism driving Pb(II) adsorption further [31–33]. The pseudo-first order equation is given as follows:

$$\log(q_e - q_t) = \log(q_e) - \frac{k_1 t}{2.303}$$

where k_1 is the rate constant of first order sorption (min^{-1}); q_e is the amount of solute sorbed at equilibrium (mg g^{-1}); q_t is the amount of solute sorbed on the surface of the sorbent at time t (mg g^{-1}).

The pseudo-second order equation is given as follows:

$$\left(\frac{t}{q_t}\right) = \left(\frac{1}{k_2 q_e^2}\right) + \left(\frac{t}{q_e}\right)$$

where k_2 is the rate constant for the pseudo second-order adsorption of Pb(II) (g mg^{-1} min^{-1}), and all variables in pseudo-second order equation are as described for pseudo-first order equation.

Fig. 9 is the plots of the linearized form of pseudo first-order and pseudo-second order model. The calculated equilibrium adsorption capacities ($Q_{e,cal}$ = 45.81 mg g^{-1}) was obtained from pseudo first-order with a low correlation coefficient (r^2 = 0.896). Whereas, the calculated equilibrium adsorption capacities ($Q_{e,cal}$ = 20.83 mg g^{-1}) estimated from pseudo-second-order kinetic model with a high correlation coefficient (r^2 = 0.990), is relatively close to the maximum adsorption capacity (Q_{eq} = 19.61 mg g^{-1}). Therefore, the adsorption system of Fe_3O_4@SiO_2@IIP toward Pb(II) is better fit to pseudo-second order model. And this adsorption mechanism is predominant for the ion-imprinted adsorbent system based on the assumption that the rate-limiting step may be chemical sorption

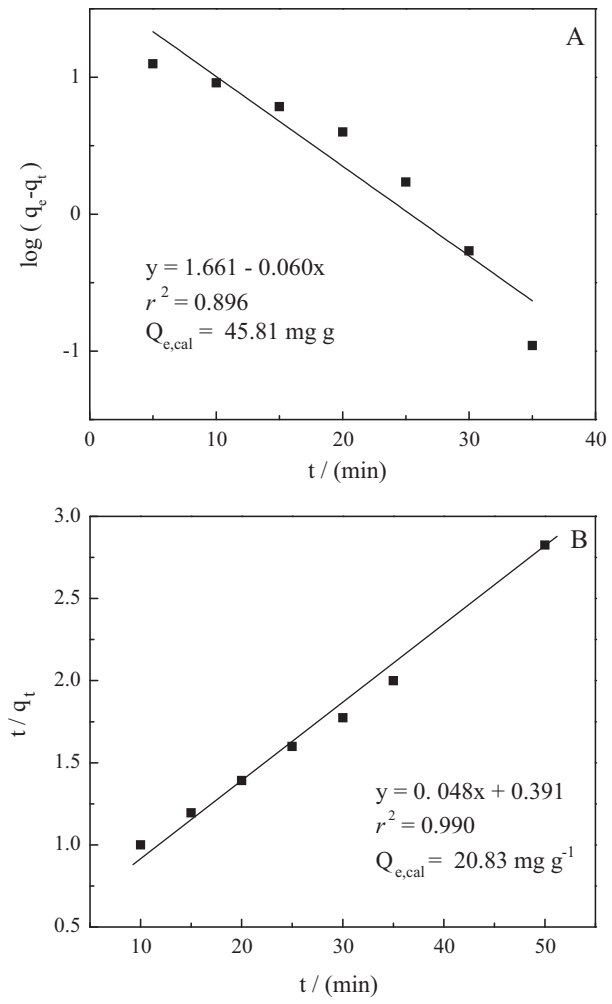

Fig. 9. A pseudo first-order kinetic isotherms (A) and a pseudo second-order kinetic isotherm (B) of Fe_3O_4@SiO_2@IIP.

between chemical binding sites on the surface of Fe_3O_4@SiO_2@IIP and Pb(II).

3.3.4. Selectivity

The selectivity of the Fe_3O_4@SiO_2@IIP toward Pb(II) was valued by competitive adsorption in the presence of various competitive metal ions. A mixture of Pb(II), Cu(II), Zn(II), Cd(II) and Hg(II) was added into deionized water to obtain an initial concentration of 10 μg mL^{-1} each for Pb(II), Cd(II), Hg(II) and Cu(II). After a competitive adsorption equilibrium reached for 1 h, the concentration of Pb(II), Cu(II), Zn(II), Cd(II) and Hg(II) in the remaining samples were detected by FAAS. The following equations were used to quantify the selectivity of Fe_3O_4@SiO_2@IIP [7,34]:

extraction percentage (%), $E = \dfrac{C_0 - C_e}{C_e}$

where C_0 and C_e are the initial and equilibrium concentration

distribution ratio (mL g^{-1}), $K = \dfrac{Q}{C_e}$

where Q is the adsorption capacity (mg g^{-1})

selectivity factor, $\alpha = \dfrac{K_t}{K_c}$

Table 1
Distribution ratio, selectivity coefficient and relative selectivity coefficient of Fe_3O_4@SiO_2@IIP and Fe_3O_4@SiO_2@NIP (Fe_3O_4@SiO_2@IIP amount 20 mg; Pb(II) 10 μg mL^{-1}; pH 7.5; sample volume of 20 mL; the washing conditions: 2 mL carbonate buffer (pH = 9); the eluting conditions: 6 mL nitric acid (0.2 mol L^{-1})).

Metal ions	Ionic charge	Ionic radii (Å)	K		α		β
			IIP[a]	NIP[b]	IIP	NIP	–
Pb	2	1.19	195.7	57.2	–	–	–
Cu	2	0.73	32.5	70.4	6.02	0.81	7.41
Zn	2	0.74	23.6	46.6	8.29	1.23	6.76
Cd	2	0.97	59.1	64.8	3.31	0.88	3.75
Hg	2	1.02	26.4	49.3	7.41	1.16	6.39

[a] Fe_3O_4@SiO_2@IIP.
[b] Fe_3O_4@SiO_2@NIP.

where K_t and K_c are the distribution ratio Pb(II) and Cu(II), Zn(II), Cd(II) or Hg(II), respectively

relative selectivity factor, $\beta = \dfrac{\alpha_i}{\alpha_n}$

where α_i and α_n are the selectivity factor of Fe_3O_4@SiO_2@IIP and Fe_3O_4@SiO_2@NIP.

As shown in Table 1, the distribution ratio and selectivity factor of the Fe_3O_4@SiO_2@IIP for Pb(II) is greater than that of the Fe_3O_4@SiO_2@NIP, which indicated the form of the imprinting effect in the imprinted shell of Fe_3O_4@SiO_2@IIP. Moreover, the distribution ratio of the Fe_3O_4@SiO_2@IIP for Pb(II) is much higher than those for other ions. The results implied that the imprinted cavities and specific binding sites in a predetermined orientation were formed. Due to high selectivity of specific binding sites toward Pb(II), the relative selectivity factors were over 3.75 by calculating in the present of Cu(II), Zn(II), Cd(II) and Hg(II).

In various real water samples, Pb(II) often accompanies with Na(I), K(I), Ca(II), Mg(II), Ni(II), Fe(II), Fe(III), Co(II) and Mn(II). The effects of these ions on the selective adsorption of Fe_3O_4@SiO_2@IIP toward Pb(II) were also studied using batch adsorption procedure. The results showed that it had no significant effect on the adsorption by adding ten times concentration of foreign ions as Pb(II).

3.4. Optimization of M-SPE procedure

Several variables including eluting concentration and volume, sample volume, will affect the performance of the extraction. In order to get the optimum extracting conditions of M-SPE procedure for separation and enrichment of Pb(II) from environmental samples, these variables were investigated.

3.4.1. Optimization of the eluting solvent

It is well known that a suitable eluent plays an important role on the extraction performance of M-SPE procedure. The interaction between Pb(II) and –NH–CH_2–CH_2–NH_2 groups could be easily destroyed by the protonation of –NH–CH_2–CH_2–NH_2 groups under strong acid conditions. In order to investigate the effect of eluent on the extraction performance, the Fe_3O_4@SiO_2@IIP was eluted by nitric acid or hydrochloric acid with concentrations ranging from 0.01 mol L^{-1} to 0.3 mol L^{-1}. The results indicated there are no significant differences when the MIP was eluted by these eluents with the same concentration. And poor elution efficiency was observed with low eluting concentration (0.01–0.05 mol L^{-1}). The increasing concentration of eluent resulted in increment in the recovery of Pb(II). And high recovery (97.8%) was obtained when the concentration of eluent is up to 0.2 mol L^{-1}. Thus, nitric acid with concentration of 0.2 mol L^{-1} was selected for further experiments.

The eluting volume ranging from 1.0 mL to 5.0 mL was studied in the eluting process. The average recovery was up to 97.8%

Table 2
Recoveries of Pb(II) in environmental samples.

Samples	Added (ng/mL)	Found (ng/mL, $n = 4$)	Recovery (%)
Tap water	0	BDL	–
	10.0	9.8 ± 0.3	98.0
	50.0	49.2 ± 0.4	98.4
Lake water	0	BDL	–
	10.0	10.1 ± 0.4	101.0
	50.0	49.7 ± 0.5	99.4
River water	0	BDL	–
	10.0	10.4 ± 0.2	104.0
	50.0	50.6 ± 0.4	101.2

BDL: below the detection limit.

with 2.0 mL eluent for three times, and no significant difference was observed with further increasing of eluting volume. Consequently, 6 mL of nitric acid (0.2 mol L^{-1}) was selected for further M-SPE experiments.

3.4.2. Optimization of sample volume

The optimization experiment of sample volume was carried out with different volumes of samples spiked with Pb(II) (1.0 μg mL^{-1}). The amount of the Fe_3O_4@SiO_2@IIP was set to 100 mg. High recoveries were obtained when the sample volume was less than 300 mL. Whereas, further increasing of sample volume resulted in decreased recovery. Due to increasing volume of the sample, the effective binding sites were masked by the complex matrix with large sample volume [34], and Pb(II) can not be absorbed fully by specific adsorption. Therefore, 300 mL was selected as the breakthrough volume.

3.5. Application

Under the optimum conditions, the M-SPE method was established for the extraction of Pb(II) from environmental samples spiked with various amounts of Pb(II). After incubated with sample solutions, the MIP materials were washed with carbonate buffer (pH = 9), and eluted with nitric acid (0.2 mol L^{-1}), the concentration of Pb(II) in the elution was detected using FAAS. As shown in Table 2, high recoveries ranged from 98.0% to 104.0% in the all tested concentration of Pb(II), which indicated that the M-SPE procedure showed a high effectivity for extracting Pb(II) from environmental water.

Reusability of Fe_3O_4@SiO_2@IIP is one of key factors in evaluating the performance of the adsorption materials. In order to investigate the reusability and stability of Fe_3O_4@SiO_2@IIP, adsorption–desorption cycle was repeated 40 times by using the same imprinted materials. The results showed that the Fe_3O_4@SiO_2@IIP is stable in operation process without loosing significantly their adsorption capacities and decrease in the recoveries of the studied target ion.

4. Conclusions

In our work, a magnetic ion-imprinted polymer based on Fe_3O_4 particles was prepared successfully by a sol-gel process. The obtained Fe_3O_4@SiO_2@IIP was well-dispersed with average size of 200 nm. This magnetic imprinted adsorbent exhibited high selectivity toward Pb(II) with the relative selectivity factor over 3.75 in the present of Cu(II), Zn(II), Cd(II) and Hg(II). When the magnetic absorbent was used in M-SPE, good recoveries (>98.0%) for Pb(II) were obtained in environmental samples under the optimized conditions. The magnetic imprinted adsorbent can be applied to rapid extraction of Pb(II) from environmental samples.

Acknowledgements

Project supported by the National Natural Science Foundation of China (No. 21005030), the Research Foundation of Education Bureau of Hunan Province, China (No. 10A099), the Plan of Western Light and the Graduate Innovation Research Fund of Jishou University (JGY201013).

References

[1] E.C. Figueiredo, D.M. Oliveira, M.E.P.B. Siqueira, M.A.Z. Arruda, On-line molecularly imprinted solid-phase extraction for the selective spectrophotometric determination of nicotine in the urine of smokers, Anal. Chim. Acta 635 (2009) 102–107.
[2] Y. Liu, H.F. Li, J.M. Lin, Magnetic solid-phase extraction based on octadecyl functionalization of monodisperse magnetic ferrite microspheres for the determination of polycyclic aromatic hydrocarbons in aqueous samples coupled with gas chromatography–mass spectrometry, Talanta 77 (2009) 1037–1042.
[3] Y.L. Liu, L. Jia, Analysis of estrogens in water by magnetic octadecylsilane particles extraction and sweeping micellar electrokinetic chromatography, Microchem. J. 89 (2008) 72–76.
[4] S.X. Zhang, H.Y. Niu, Z.J. Hu, Y.Q. Cai, Y.L. Shi, Preparation of carbon coated Fe_3O_4 nanoparticles and their application for solid-phase extraction of polycyclic aromatic hydrocarbons from environmental water samples, J. Chromatogr. A 1217 (2010) 4757–4764.
[5] L.G. Chen, X.P. Zhang, L. Sun, Y. Xu, Q.L. Zeng, H. Wang, H.Y. Xu, A.M. Yu, H.Q. Zhang, L. Ding, Fast and selective extraction of sulfonamides from honey based on magnetic molecularly imprinted polymer, J. Agric. Food Chem. 57 (2009) 10073–10080.
[6] Y.H. Deng, D.W. Qi, C.H. Deng, X.M. Zhang, D.Y. Zhao, Superparamagnetic high-magnetization microspheres with an Fe_3O_4@SiO_2 core and perpendicularly aligned mesoporous SiO_2 shell for removal of microcystins, J. Am. Chem. Soc. 130 (2008) 28–29.
[7] C.J. Tan, Y.W. Tong, Preparation of superparamagnetic ribonuclease a surface-imprinted submicrometer particles for protein recognition in aqueous media, Anal. Chem. 79 (2007) 299–306.
[8] S.H. Xuan, Y.X.J. Wang, K.C.F. Leung, K.Y. Shu, Synthesis of Fe_3O_4@polyaniline core/shell microspheres with well-defined blackberry-like morphology, J. Phys. Chem. C 112 (2008) 18804–18809.
[9] N. Frickel, R. Messing, T. Gelbrich, A.M. Schmidt, Functional silanes as surface modifying primers for the preparation of highly stable and well-defined magnetic polymer hybrids, Langmuir 26 (2010) 2839–2846.
[10] X.W. Kan, Q. Zhao, D.L. Shao, Z.R. Geng, Z.L. Wang, J.J. Zhu, Preparation and recognition properties of bovine hemoglobin magnetic molecularly imprinted polymers, J. Phys. Chem. B 114 (2010) 3999–4004.
[11] X.H. Gu, R. Xu, G.L. Yuan, H. Lu, B.R. Gu, H.P. Xie, Preparation of chlorogenic acid surface-imprinted magnetic nanoparticles and their usage in separation of Traditional Chinese Medicine, Anal. Chim. Acta 675 (2010) 64–70.
[12] Y. Li, X. Li, J. Chu, C.K. Dong, J.Y. Qi, Y.X. Yuan, Synthesis of core–shell magnetic molecular imprinted polymer by the surface RAFT polymerization for the fast and selective removal of endocrine disrupting chemicals from aqueous solutions, Environ. Pollut. 158 (2010) 2317–2323.
[13] Y. Li, C.K. Dong, J. Chu, J.Y. Qi, X. Li, Surface molecular imprinting onto fluorescein-coated magnetic nanoparticles via reversible addition fragmentation chain transfer polymerization: a facile three-in-one system for recognition and separation of endocrine disrupting chemicals, Nanoscale 3 (2011) 280–287.
[14] W.L. Guo, W. Hu, J.M. Pan, H.C. Zhou, W. Guan, X. Wang, J.D. Dai, L.C. Xu, Selective adsorption and separation of BPA from aqueous solution using novel molecularly imprinted polymers based on kaolinite/Fe_3O_4 composites, Chem. Eng. J. 171 (2011) 603–611.
[15] J.M. Pan, H. Yao, W. Guan, H.X. Ou, P.W. Huo, X. Wang, X.H. Zou, C.X. Li, Selective adsorption of 2 6-dichlorophenol by surface imprinted polymers using polyaniline/silica gel composites as functional support: equilibrium, kinetics, thermodynamics modeling, Chem. Eng. J. 172 (2011) 847–855.
[16] R.G.C. Silva, F. Augusto, Sol–gel molecular imprinted ormosil for solid-phase extraction of methylxanthines, J. Chromatogr. A 1114 (2006) 216–223.
[17] G.Z. Fang, J. Tan, X.P. Yan, An ion-imprinted functionalized silica gel sorbent prepared by a surface imprinting technique combined with a sol–gel process for selective solid-phase extraction of cadmium(II), Anal. Chem. 77 (2005) 1734–1739.
[18] T.P. Rao, S. Daniel, J.M. Gladis, Tailored materials for preconcentration or separation of metals by ion-imprinted polymers for solid-phase extraction (IIP-SPE), Trends Anal. Chem. 23 (2004) 28–35.
[19] X. Luo, S. Luo, Y. Zhan, H. Shu, Y. Huang, X. Tu, Novel Cu (II) magnetic ion imprinted materials prepared by surface imprinted technique combined with a sol–gel process, J. Hazard. Mater. 192 (2011) 949–955.
[20] Y.M. Ren, M.L. Zhang, D. Zhao, Synthesis and properties of magnetic Cu(II) ion imprinted composite adsorbent for selective removal of copper, Desalination 228 (2008) 135–149.
[21] N. Candan, N. Tüzmen, M. Andac, C.A. Andac, R. Say, A. Denizli, Cadmium removal out of human plasma using ion-imprinted beads in a magnetic column, Mater. Sci. Eng. C 29 (2009) 144–152.

[22] J. Tan, H.F. Wang, X.P. Yan, A fluorescent sensor array based on ion imprinted mesoporous silica, Biosens. Bioelectron. 24 (2009) 3316–3321.
[23] G.Z. Fang, J. Tan, X.P. Yan, An ion-imprinted functionalized silica gel sorbent prepared by a surface imprinting technique combined with a sol gel process for selective solid-phase extraction of cadmium(II), Anal. Chem. 77 (2005) 1734–1739.
[24] Z.H. Zhang, H.B. Zhang, Y.G. Hu, S.Z. Yao, Synthesis and application of multi-walled carbon nanotubes—molecularly imprinted sol–gel composite material for on-line solid-phase extraction and high-performance liquid chromatography determination of trace Sudan IV, Anal. Chim. Acta 661 (2010) 173–180.
[25] Y.K. Lu, X.P. Yan, An imprinted organic inorganic hybrid sorbent for selective separation of cadmium from aqueous solution, Anal. Chem. 76 (2004) 453–457.
[26] Z.T. Zhang, S. Saengkerdsub, S. Dai, Intersurface ion-imprinting synthesis on layered magadiite hosts, Chem. Mater. 15 (2003) 2921–2925.
[27] F. Zheng, B. Hu, Preparation of a high pH-resistant AAPTS-silica coating and its application to capillary microextraction (CME) of Cu, Zn, Ni, Hg and Cd from biological samples followed by on-line ICP-MS detection, Anal. Chim. Acta 605 (2007) 1–10.
[28] X.B. Zhu, Y.M. Cui, X.J. Chang, X.J. Zou, Z.H. Li, Selective solid-phase extraction of lead(II) from biological and natural water samples using surface-grafted lead(II)-imprinted polymers, Microchim. Acta 164 (2009) 125–132.
[29] H.B. Hu, Z.H. Wang, L. Pan, Synthesis of monodisperse Fe_3O_4@silica core–shell microspheres and their application for removal of heavy metal ions from water, J. Alloys Compd. 492 (2010) 656–661.
[30] M.T. Jafari, B. Rezaei, B. Zaker, Ion mobility spectrometry as a detector for molecular imprinted polymer separation and metronidazole determination in pharmaceutical and human serum samples, Anal. Chem. 81 (2009) 3585–3591.
[31] Y.S. Ho, G. McKay, Pseudo-second order model for sorption processes, Process Biochem. 34 (1999) 451–456.
[32] C.Y. Chen, C.Y. Yang, A.H. Chen, Biosorption of Cu(II), Zn(II), Ni(II) and Pb(II) ions by cross-linked metal-imprinted chitosans with epichlorohydrin, J. Environ. Manage. 92 (2011) 796–802.
[33] E. Birlik, A. Ersöz, A. Denizli, R. Say, Preconcentration of copper using double-imprinted polymer via solid phase extraction, Anal. Chim. Acta 565 (2006) 145–151.
[34] Y.W. Liu, X.J. Chang, S. Wang, Y. Guo, B.J. Din, S.M. Meng, Solid-phase extraction and preconcentration of cadmium(II) in aqueous solution with Cd(II)-imprinted resin (poly-Cd(II)-DAAB-VP) packed columns, Anal. Chim. Acta 519 (2004) 173–179.